PHYSICAL REVIEW C

NUCLEAR PHYSICS

THIRD SERIES, VOLUME 30, NUMBER 4 OCTOBER 1984

Configuration space Faddeev continuum calculations: N-d s-wave scattering lengths with tensor-force interactions

J. L. Friar and B. F. Gibson
Theoretical Division, Los Alamos National Laboratory, Los Alamos, New Mexico 87545

G. L. Payne and C. R. Chen
Department of Physics and Astronomy, University of Iowa, Iowa City, Iowa 52242
(Received 19 June 1984)

Formulation of the s-wave, zero-energy Faddeev-type scattering equations for a model which includes a spin-triplet tensor-force nucleon-nucleon interaction and a Coulomb force between two protons is discussed. Numerical solution of the equations for the Reid-soft-core, Argonne V_{14}, and super-soft-core C potential models is obtained using spline techniques. Kohn variational estimates are also presented, and comparison is made with other previously published results. The inclusion of a tensor force does not alter our previous conclusions about the Coulomb force effects on the p-d scattering length, which were based upon s-wave nucleon-nucleon potential model studies.

I. INTRODUCTION

Solving exact few-body equations allows us to test our understanding of nuclear forces by direct comparison of model calculations with experimental data and to probe for novel features of physical observables. Trinucleon bound-state investigations have yielded interesting examples in each of these categories.[1] Nonetheless, it is the scattering problem which provides the real opportunity to explore in depth the accuracy of our knowledge of the nucleon-nucleon interaction. Neutron-deuteron (nd) elastic scattering at zero incident energy is the simplest such three-nucleon scattering problem. However, it is now clear that the value of the nd doublet scattering length ($^2a_{\rm nd}$) is closely coupled to the value of the triton binding energy [$B(^3{\rm H})$] and that the nd quartet scattering length ($^4a_{\rm nd}$) is determined primarily by the properties of the deuteron pole.[2,3] The situation with respect to proton-deuteron (pd) scattering is not as clear. In particular, the size of the Coulomb modification of the quartet scattering length was found to be much larger in s-wave potential, Faddeev-type calculations[3,4] than in approximate calculations which reduce the procedure to an effective two-particle problem. We also found, in our s-wave nucleon-nucleon force calculations,[3] the pd doublet scattering length ($^2a_{\rm pd}$) to be much smaller than $^2a_{\rm nd}$, in disagreement with the established relationship[5] between $^2a_{\rm nd}$ and $B(^3{\rm H})$. [Model calculations employing short-range two-body forces show that $^2a_{\rm nd}$ increases as $B(^3{\rm H})$ increases, assuming $B(^2{\rm H})$ is reproduced by the potential model.] Thus, we are led to investigate the zero-energy Nd scattering problem with tensor force NN interactions in order to test the general validity of our findings.

The accepted experimental values for the nd scattering lengths are[6]

$$^4a_{\rm nd}=6.35\pm0.02 \text{ fm},$$

$$^2a_{\rm nd}=0.65\pm0.04 \text{ fm}.$$

These are obtained by extrapolation of low-energy cross section data to zero energy. Because there exists a pole close to zero energy, the radius of convergence of the usual effective range expansion is very small,[7–11] which originally led to some confusion as to the proper value for $^2a_{\rm nd}$.[6,9,12] This small radius of convergence results not from the ground state pole but from the virtual bound-state singularity, which lies on the second sheet of the energy plane. We note that this virtual bound state, whose analytic properties are analogous to those of the spin-singlet deuteron in the neutron-proton system, will migrate onto the first sheet in any model calculation in which the nucleon-nucleon forces become strong enough to support a particle-stable excited state in the trinucleon system. Therefore, it should be reasonable to expect that the Coulomb interaction in the ^{3}He-$^2a_{\rm pd}$ problem will move the virtual state of the ^{3}He farther from the origin than it is in the ^{3}H case, perhaps even removing it from the region where it has a significant effect upon the expansion for the proton-deuteron doublet scattering amplitude. Experimentally, there is some support for this speculation,[13] but we shall not explore it further in this paper. Additional singularities, such as branch cuts, are

also expected in the p-d problem. It was in part the established relationship between the ^{3}H binding energy and the nd doublet scattering length that led to general acceptance of the s-wave proton-deuteron doublet and quartet scattering length values first determined from extrapolation of the phase shifts extracted from analysis of the available low-energy pd elastic scattering data:[9,14]

$$^4a_{\rm pd}=11.88^{+0.4}_{-0.1}\ {\rm fm}\ ,$$

$$^2a_{\rm pd}=2.73\pm0.10\ {\rm fm}\ .$$

Recently the Giessen group[13] reported values for these scattering lengths which are not qualitatively different:

$$^4a_{\rm pd}=11.11\pm0.25\ ,$$

$$^2a_{\rm pd}=4.00^{+1.00}_{-0.67}\ .$$

The sign and approximate magnitude of the quartet difference $^4a_{\rm pd}-{}^4a_{\rm nd}$ were reproduced by several theoretical calculations: the Jost function analysis of Timm and Stingl,[15] the dispersion relation analysis of Eyre, Phillips, and Roig,[16] and the approximation procedure of Avishai and Rinat.[17] The s-wave separable potential estimate of $^4a_{\rm pd}=13.3$ fm by Alt[4] using the Alt-Grassberger-Sandhas (AGS) formalism[18] was the only theoretical estimate of that quantity which was significantly larger than the quoted experimental value prior to our own s-wave potential calculations.[1] The estimates of the pd doublet scattering length made in Refs. 16 and 17 also agreed qualitatively with the quoted experimental value, implying a large increase in the magnitude of the Nd doublet scattering length in the presence of a Coulomb force. However, our configuration space Faddeev equation calculations based upon (partial-wave) local s-wave nucleon-nucleon interactions sharply disagreed with experiment and all of the theoretical studies except the $^4a_{\rm pd}$ result of Alt. In particular, we found (1) $^4a_{\rm pd}$ to be approximately 14 fm and (2) $^2a_{\rm pd}$ to be approximately zero. The later work of Kvitsinski[19] is also in contradiction to our s-wave potential results. However, the qualitative studies of Zankel and Mathelitsch[20] confirm our findings. Thus, it should be readily apparent why we wished to explore the Nd scattering length problem in terms of tensor force nucleon-nucleon potentials. In fact, we find the tensor force model results to be in essential agreement with our s-wave potential calculation. Hence, our pd conclusions remain unchanged, and we believe that $^4a_{\rm pd}$ is approximately 13.5—14.0 fm while $^2a_{\rm pd}$ is very small. This latter finding is indeed contrary to the intuition based upon experience with the Phillips line[5] for $B(^3{\rm H})$ vs $^2a_{\rm nd}$. That is, we find $^2a_{\rm pd}$ to be smaller than $^2a_{\rm nd}$ rather than larger, even though $B(^3{\rm He})$ is smaller than $B(^3{\rm H})$. Therefore, this novel feature of the "Coulomb correction" to the doublet scattering length provides another example of how exact calculations are sometimes required in order to provide a complete understanding of the physics of nuclear systems.

In Sec. II of this paper we outline the three-body scattering equations in configuration space when tensor forces are involved. We work in configuration space because the long-range Coulomb force is naturally introduced in that space. We also discuss the problem of numerically solving the resulting partial-wave equations. In Sec. III we present our numerical results for the Faddeev equations as well as Kohn variational[21] estimates. We also compare with previously published values. We summarize our conclusions in Sec. IV.

II. CONFIGURATION SPACE EQUATIONS

A. Formal structure

The motivation for Faddeev's revolutionary work[22] on the t-matrix approach to the three-body scattering problem arose from the fact that the boundary conditions in a Lippmann-Schwinger equation formulation of the scattering problem are ill defined. The Faddeev decomposition (or its equivalent) of the scattering amplitude provides a convenient method of enforcing the proper boundary conditions required to obtain a unique solution. Noyes first outlined the configuration space boundary condition problem for nd scattering.[23] The Grenoble group developed the configuration space Faddeev equation approach to the point of numerical solution.[24] Including the long range Coulomb interaction is a nontrivial addition. Redish suggested modifying the Faddeev equations so that the effective interaction is of short range;[25] Sasakawa and Sawada studied a particular Coulomb potential modification.[26] We chose in Ref. 1 to utilize the approach that we adopted in our bound state asymptotic normalization calculations.[27] Kvitsinski based his calculations upon the formalism of Merkuriev.[28] Thus there is a long history to the configuration space Faddeev equations. We review here briefly their structure and the Coulomb modifications we employ.

The Faddeev equations which describe three nucleons interacting via realistic two-body potentials have the same form whether one is investigating the bound state or the scattering problem. However, the boundary conditions for these two problems differ considerably.[3,23,24] In the bound state problem the wave function vanishes asymptotically, and the solution is insensitive to details of implementing this boundary condition. For the scattering problem the wave function is nonzero in the asymptotic region, and numerical solution of the Faddeev equations is much more sensitive to the specific boundary conditions. In addition, because the continuum wave function remains finite for large values of the relative coordinates, it is necessary to ensure accurate solutions for these regions as well as those which are significant for the bound state problem. Consequently, in order to make the calculation tractable it is important to extract from the wave function as much of the asymptotic structure as possible prior to numerical solution. The resulting (unknown) function is much smoother; it can therefore be accurately approximated by a smaller number of basis functions.

We first review the Faddeev equations for three nucleons in the j-J coupling scheme. We then derive the equations for the smoother, auxiliary function from which the known asymptotic structure has been removed. The total wave function Ψ is decomposed into a sum of the three Faddeev amplitudes

$$\Psi=\Psi_1(\vec{x}_1,\vec{y}_1)+\Psi_2(\vec{x}_2,\vec{y}_2)+\Psi_3(\vec{x}_3,\vec{y}_3)\ , \tag{1}$$

where $\vec{x}_i$ and $\vec{y}_i$ are the Jacobi coordinates

$$\vec{x}_i=\vec{r}_j-\vec{r}_k \tag{2a}$$

and

$$\vec{y}_i=\tfrac{1}{2}(\vec{r}_j+\vec{r}_k)-\vec{r}_i \tag{2b}$$

for three nucleons having coordinates $\vec{r}_1$, $\vec{r}_2$, and $\vec{r}_3$. The Schrödinger equation

$$\left[T+\sum_i V(\vec{x}_i)+\sum_i V_C(x_i)-E\right]\Psi=0 \tag{3}$$

can be decomposed into the three coupled Faddeev equations

$$[T+V(\vec{x}_i)+V_C(x_1)+V_C(x_2)+V_C(x_3)-E]\Psi_i(\vec{x}_i,\vec{y}_i)=-V(\vec{x}_i)[\Psi_j(\vec{x}_j,\vec{y}_j)+\Psi_k(\vec{x}_k,\vec{y}_k)]\ , \tag{4}$$

where T is the kinetic energy operator, $V(\vec{x}_i)$ is the nuclear two-body interaction, and

$$V_C(x_i)=\frac{e^2}{x_i}\frac{[1+\tau_z(j)][1+\tau_z(k)]}{4} \tag{5}$$

is the two-body Coulomb interaction. Note that we have retained the entire Coulomb potential on the left-hand side of Eq. (4), which minimizes the long-range Coulomb polarization distortions. In previous calculations[26,27] involving Coulomb potentials, the two-body Coulomb force was treated in the same manner as the nuclear force. This required the addition and subtraction of distorting potentials. Such an approach was also tried for the present problem, where it was found that the distorting potentials caused numerical difficulties in the asymptotic region. The method characterized in Eq. (4) was found to be the most stable for numerical calculations.

B. Numerical solution

For three identical nucleons, it is only necessary to solve one of the three equations in Eq. (4); all three Faddeev amplitudes have the same functional form. In making a partial wave expansion of the Faddeev amplitude we use the j-J coupling scheme and write the wave function in the form

$$\Psi_1(\vec{x}_1,\vec{y}_1)=\sum_\alpha \frac{\psi_\alpha(x_1,y_1)}{x_1y_1}\,|\alpha\rangle\ , \tag{6}$$

where

$$|\alpha\rangle=|[(l_\alpha,s_\alpha)j_\alpha,(L_\alpha,S_\alpha)J_\alpha]\mathscr{J}\mathscr{M};(t_\alpha,T_\alpha)\mathscr{T}\mathscr{M}_T\rangle\ , \tag{7}$$

l_α is the relative orbital angular momentum of particles 2 and 3, s_α is the spin angular momentum of particles 2 and 3, j_α is the total angular momentum of particles 2 and 3, L_α is the orbital angular momentum of particle 1 relative to the center of mass of particles 2 and 3, S_α is the spin of particle 1 ($S_\alpha=\frac{1}{2}$), J_α is the total angular momentum of particle 1, $\mathscr{J}$ is the total angular momentum ($\mathscr{J}=\frac{1}{2},\frac{3}{2}$), t_α is the isospin of particles 2 and 3, T_α is the isospin of particle 1, and $\mathscr{T}$ is the total isospin ($T_\alpha=\mathscr{T}=\frac{1}{2}$).

We consider the case of local nucleon-nucleon interactions acting only in the $^1S_0$ and $^3S_1$-$^3D_1$ states. For this situation only the five states listed in Table I are needed to describe the doublet amplitude for zero energy scattering, and only the seven states listed in Table II are needed to describe quartet scattering. ($\mathscr{L}$ and $\mathscr{S}$ are the total orbital angular momentum and spin in $\mathscr{L}$-$\mathscr{S}$ coupling.) To obtain the coupled equations for the channel wave functions, we multiply Eq. (4) by $-x_1y_1M/\hbar^2$, take the inner product with $\langle\alpha|$, and transform to the hyperspherical variables defined by

$$x_1=\rho\cos\theta \tag{8a}$$

and

$$y_1=\frac{\sqrt{3}}{2}\rho\sin\theta\ . \tag{8b}$$

The resulting equations are

$$(\Delta_\alpha-\kappa^2)\psi_\alpha(\rho,\theta)-\sum_{\alpha'}(v_{\alpha\alpha'}+v^C_{\alpha\alpha'})\Psi_{\alpha'}(\rho,\theta)-\sum_{\alpha''}v_{\alpha\alpha''}\sum_{\alpha'}\int_{\theta^-}^{\theta^+}d\theta' K_{\alpha''\alpha'}(\theta,\theta')\psi_{\alpha'}(\rho,\theta')=0\ , \tag{9}$$

where we have defined

$$v_{\alpha\alpha'}=\frac{M}{\hbar^2}\langle\alpha\,|\,V(\vec{x}_1)\,|\,\alpha'\rangle\ , \tag{10a}$$

$$v^C_{\alpha\alpha'}=\frac{M}{\hbar^2}\langle\alpha\,|\,V_C(x_1)+V_C(x_2)+V_C(x_3)\,|\,\alpha'\rangle\ , \tag{10b}$$

$$\sum_{\alpha'}\int_{\theta^-}^{\theta^+}d\theta' K_{\alpha''\alpha'}(\theta,\theta')\psi_{\alpha'}(\rho,\theta')=x_1y_1\langle\alpha''\,|\,\Psi(\vec{x}_2,\vec{y}_2)+\Psi(\vec{x}_3,\vec{y}_3)\rangle\ , \tag{10c}$$

$$E=-\frac{\hbar^2\kappa^2}{M}\ , \tag{10d}$$

and

$$\Delta_\alpha=\frac{\partial^2}{\partial\rho^2}+\frac{1}{\rho}\frac{\partial}{\partial\rho}+\frac{1}{\rho^2}\frac{\partial^2}{\partial\theta^2}-\frac{l_\alpha(l_\alpha+1)}{\rho^2\cos^2\theta}-\frac{L_\alpha(L_\alpha+1)}{\rho^2\sin^2\theta}\ . \tag{10e}$$

TABLE I. The five three-body Faddeev amplitudes comprising the doublet scattering length solution when the NN interaction is restricted to ($^1S_0$,$^3S_1$-$^3D_1$): Total $\mathscr{J}=\mathscr{T}=\frac{1}{2}$.

$(l_\alpha,s_\alpha)j_\alpha$	$(L_\alpha,S_\alpha)J_\alpha$	t_α	$\mathscr{L}$	$\mathscr{S}$
(0,0)0	$(0,\frac{1}{2})\frac{1}{2}$	1	0	$\frac{1}{2}$
(0,1)1	$(0,\frac{1}{2})\frac{1}{2}$	0	0	$\frac{1}{2}$
(2,1)1	$(0,\frac{1}{2})\frac{1}{2}$	0	2	$\frac{3}{2}$
(0,1)1	$(2,\frac{1}{2})\frac{3}{2}$	0	2	$\frac{3}{2}$
(2,1)1	$(2,\frac{1}{2})\frac{3}{2}$	0	0,1,2	$\frac{1}{2},\frac{3}{2}$

The integration limits θ^- and θ^+ are the same as for the bound state calculations,[29] and for zero-energy scattering, κ is the two-body bound-state wave number. However, $K_{\alpha\beta}$ is *not* identical to the kernel defined in Ref. 29.

As discussed above, we simplify the numerical calculations by writing ψ_α in the form

$$\psi_\alpha(x_1,y_1)=\phi_\alpha(x_1,y_1)+\Omega_\alpha(x_1,y_1)\ , \tag{11}$$

where ϕ_α is the incident wave. For $L_\alpha>0$ or $(l_\alpha,s_\alpha)j_\alpha\neq(0,1)1$ or (2,1)1 then $\phi_\alpha=0$. For the open channels,

$$\phi_\alpha(x_1,y_1)=y_1\mathscr{F}(z)u_d(x_1)\ . \tag{12}$$

Here $u_d(x_1)$ is the reduced deuteron bound-state wave function and $\mathscr{F}(z)$ can be expressed in terms of a modified Bessel function of order 1:

$$\mathscr{F}(z)=z^{-1/2}I_1(2\sqrt{z})\ . \tag{13}$$

The quantity $z=2\alpha\mu y_1$ in the argument depends upon the fine structure constant, α, and the reduced mass, μ.

Inserting Eq. (11) into Eq. (9) one obtains the following equations for the reduced scattering function Ω_α:

$$(\Delta_\alpha-\kappa^2)\Omega_\alpha(\rho,\theta)-\sum_{\alpha'}(v_{\alpha\alpha'}+v^C_{\alpha\alpha'})\Omega_{\alpha'}(\rho,\theta)-\sum_{\alpha''}v_{\alpha\alpha''}\sum_{\alpha'}\int_{\theta^-}^{\theta^+}d\theta' K_{\alpha''\alpha'}(\theta,\theta')\Omega_{\alpha'}(\rho,\theta')$$
$$=\sum_{\alpha'}(v^C_{\alpha\alpha'}-\omega\delta_{\alpha\alpha'})\phi_{\alpha'}(\rho,\theta)+\sum_{\alpha''}v_{\alpha\alpha''}\sum_{\alpha'}\int_{\theta^-}^{\theta^+}d\theta' K_{\alpha''\alpha'}(\theta,\theta')\phi_{\alpha'}(\rho,\theta')\ , \tag{14}$$

where

$$\omega=\frac{M}{\hbar^2}\frac{e^2}{y_1}\ . \tag{15}$$

For large values of y_1 the outgoing wave Ω_α has the asymptotic form

$$\Omega_\alpha(x_1,y_1)\underset{y_1\to\infty}{\to}-a_\alpha\mathscr{H}_\alpha(y_1)u_d(x_1) \tag{16}$$

for the deuteron channels, where

$$\mathscr{H}_\alpha(z)=\frac{(2\alpha m)^{L_\alpha}}{(2L_\alpha)!}(2\sqrt{z})K_{2L_\alpha+1}(2\sqrt{z}) \tag{17}$$

and $K_{2L_\alpha+1}$ is the modified Bessel function.

For the closed channels the function Ω_α approaches zero in the asymptotic region. In order to simplify the numerical calculations we express Ω_α in terms of the smoother auxiliary function F_α which is defined by

$$\Omega_\alpha(x_1,y_1)=F_\alpha(\rho,\theta)[y_1^{L_\alpha}\mathscr{H}_\alpha(y_1)]\frac{u_d(x_1)}{x_1} \tag{18a}$$

for the deuteron channels and

$$\Omega_\alpha(x_1,y_1)=F_\alpha(\rho,\theta)e^{-\kappa\rho} \tag{18b}$$

for the remaining channels. In Eq. (18a) we have included the factor $y_1^{L_\alpha}$ to remove the singular behavior of $\mathscr{H}_\alpha(y_1)$ at $y_1=0$. In addition, we have included the factor of $1/x_1$ in Eq. (18a) to simplify the boundary conditions at $x_1=0$.

Because Ω_α is the reduced wave function, the boundary conditions for $F_\alpha(\rho,\theta)$ are

$$F_\alpha(0,\theta)=F_\alpha(\rho,0)=F_\alpha(\rho,\pi/2)=0 \tag{19}$$

for all channels,

$$F_\alpha(\rho,\theta)\underset{y_1\to\infty}{\to}-a_\alpha\frac{x_1}{y_1^{L_\alpha}}=A(\theta)\rho^{1-L_\alpha} \tag{20a}$$

for the deuteron channels, and

$$F_\alpha(\rho,\theta)\underset{\rho\to\infty}{\to}\text{constant} \tag{20b}$$

for the nondeuteron channels. These boundary conditions are implemented by requiring that at $\rho=\rho_{\max}$,

$$\frac{\partial F_\alpha}{\partial\rho}=\frac{(1-L_\alpha)}{\rho}F_\alpha \tag{21a}$$

for the deuteron channels, and

TABLE II. The seven three-body Faddeev amplitudes comprising the quartet scattering length solution when the NN interaction is restricted to ($^1S_0$,$^3S_1$-$^3D_1$): Total $\mathscr{J}=\frac{3}{2}$,$\mathscr{T}=\frac{1}{2}$.

$(l_\alpha,s_\alpha)j_\alpha$	$(L_\alpha,S_\alpha)J_\alpha$	t_α	$\mathscr{L}$	$\mathscr{S}$
(0,1)1	$(0,\frac{1}{2})\frac{1}{2}$	0	0	$\frac{3}{2}$
(2,1)1	$(0,\frac{1}{2})\frac{1}{2}$	0	2	$\frac{1}{2},\frac{3}{2}$
(0,0)0	$(2,\frac{1}{2})\frac{3}{2}$	1	2	$\frac{1}{2},\frac{3}{2}$
(0,1)1	$(2,\frac{1}{2})\frac{3}{2}$	0	2	$\frac{1}{2},\frac{3}{2}$
(2,1)1	$(2,\frac{1}{2})\frac{3}{2}$	0	0,1,2,3	$\frac{1}{2},\frac{3}{2}$
(0,1)1	$(2,\frac{1}{2})\frac{5}{2}$	0	2	$\frac{1}{2},\frac{3}{2}$
(2,1)1	$(2,\frac{1}{2})\frac{5}{2}$	0	0,1,2,3	$\frac{1}{2},\frac{3}{2}$

$$\frac{\partial F_\alpha}{\partial \rho}=0 \tag{21b}$$

for the nondeuteron channels.

Substituting the expression for Ω_α given in Eq. (18) into Eq. (14) yields a set of coupled differential equations for the $F_\alpha(\rho,\theta)$. To solve these equations we use a bicubic spline expansion

$$F_\alpha(\rho,\theta)=\sum_{i,j} a_{ij}^\alpha s_i(\rho)s_j(\theta)\ , \tag{22}$$

where the spline functions were chosen to be the cubic Hermite splines.[30] We solve for the unknown coefficients a_{ij}^α by the technique of orthogonal collocation.[30]

III. NUMERICAL RESULTS

In our tensor force investigation of the Nd zero-energy scattering lengths, we have employed three different nucleon-nucleon potential models: (1) the Reid soft-core (RSC) potential,[31] (2) the Argonne V_{14} potential,[32] and (3) the super-soft-core C (SSCC) potential.[33]

Comparison of the numerical results for these three potentials provides an indication of the model dependence of our calculation and conclusions. The RSC model has a stiff Yukawa core (strong short-range repulsion), the V_{14} model has a moderate-strength Woods-Saxon core, and the SSCC model has a soft exponential core (weak short-range repulsion). In addition to exhibiting a repulsive strength intermediate to that of the RSC and SSCC models, the V_{14} spin-singlet parameters were fitted to the np phase shift data rather than the pp data. Thus, the V_{14} $^1S_0$ potential should be more attractive than that of the RSC or SSCC models. We list in Table III the deuteron and triton bound state energies and small wave function component probabilities generated with each of these tensor force interactions. For the RSC model, we also list the triton results for the three-channel approximation, truncating to the first three states of Table I. We shall utilize this approximate model in our investigation of the relation between $B(^3\mathrm{H})$ and $^2a_{\mathrm{nd}}$ as a function of the strength of the spin-singlet ($^1S_0$) potential. We note in passing the well-known increase in $B(^3\mathrm{H})$ as $P_D(^2\mathrm{H})$ decreases and that fact that $P_D(^3\mathrm{H})$ tracks $P_D(^2\mathrm{H})$. The value of $\hbar^2/M$ used for each model is also listed in Table III.

Because the RSC model has the strongest short-range repulsion and produces the largest bound-state D-state probabilities, we consider this model in the greatest detail. It should provide the most stringent test of accuracy and convergence in our scattering length calculations. To this end we list in Table IV the mesh parameter values for a selection of test cases which we explored in the case of the quartet scattering lengths. The corresponding $^4a_{\mathrm{nd}}$ and $^4a_{\mathrm{pd}}$ values are compiled in Table V. We quote both the value extracted from the Faddeev wave function and the Kohn variational estimate (superscript K) based upon that wave function and the channel-projected Coulomb interaction. The $^4a_{\mathrm{pd}}^{K,F}$ results follow from the same Kohn calculation without the s-wave projection. That is, we include all of the higher partial waves of the Coulomb potential in that estimate. Therefore, $^4a_{\mathrm{pd}}^{K,F}$ is the best estimate of the physical pd quartet scattering length, but the comparison of $^4a^K$ with ^4a is the proper consistency check.

As has been true in our previous bound-state and continuum wave function investigations, the sensitivity of the solution to the ρ-grid parameters is the more complex. We have added an additional break point at 0.5 fm in order to optimally distribute the points in the interior where the interaction is repulsive, while ensuring a sufficient number of points in the intermediate region interior to where the solution becomes reasonably smooth (about 12 fm). At least three points were needed in the interior (0—0.5 fm), whereas approximately ten were needed in the midrange, where the nonuniform spacing is controlled by the scale factor S_ρ. ($S_\rho=1.3$ was reasonable.) In the exterior region, we found a uniform spacing of as much as 8 fm provided a satisfactory spline distribution. Somewhat surprisingly we found it necessary to go out to $\rho_{\max}=92$ fm in order to obtain proper agreement between $^4a_{\mathrm{nd}}$ and $^4a_{\mathrm{nd}}^K$ as well as $^4a_{\mathrm{pd}}$ and $^4a_{\mathrm{pd}}^K$. Sensitivity to the θ grid was similar to that of the s-wave central force model.[1,2] However, we used a uniform distribution of points between $\theta=0$ and $\pi/6$ while scaling the points between $\pi/6$ and $\pi/2$ in order to ensure that points were concentrated in the region with the most structure in the solution. At least three θ points were required in the exterior region, where the solution decays exponentially. We needed at least 21 points in the scaled region and $S_\theta=1.35$ appeared optimal.

It is clear that the Kohn variational bounds ($^4a_{\mathrm{nd}}^K=6.31$ fm and $^4a_{\mathrm{pd}}^K=13.33$ fm) are excellent values even when the wave function solutions are not as good. A second interesting feature of the quartet results shown in Table V is that the two-channel calculation results differ insignificantly from the three-, five-, and seven-channel results (but require much less computational time). That is, one need only consider the first two channels in Table II when studying Nd quartet scattering lengths; the deuteron pole controls the quartet scattering length. A third point is that these RSC quartet scattering length results are very close to the s-wave potential results of Alt[4] and our exponential potential calculations,[1] both of which were NN

TABLE III. Deuteron and triton bound state properties for tensor force potential models investigated here.

Model	Ref.	$\hbar^2/M$	$B(^2\mathrm{H})$	$P_D(^2\mathrm{H})$	$B(^3\mathrm{H})$	$P_{S'}(^3\mathrm{H})$	$P_D(^3\mathrm{H})$	Channels
RSC	31	41.47			6.38	1.90	8.01	3
			2.2246	6.47				
RSC	31	41.47			7.02	1.67	9.34	5
V_{14}	32	41.473 14	2.2249	6.08	7.44	1.36	8.86	5
SSCC	33	41.47	2.2241	5.45	7.46	1.40	7.96	5

TABLE IV. Mesh parameters employed in the accuracy and convergence study of the Nd quartet scattering length calculations using the RSC potential model.

Case	N_I^ρ	N_M^ρ	N_E^ρ	$\rho_{\rm br}$	$\rho_{\rm br}^I$	$\rho_{\rm max}^E$	S_ρ	N_I^θ	N_E^θ	S_θ
1	3	9	5	0.5	12.	60.	1.3	18	2	1.35
2	3	10	8	0.5	12.	76.	1.3	21	2	1.35
3	3	10	8	0.5	12.	76.	1.3	20	3	1.35
4	4	12	8	0.5	12.	76.	1.3	21	2	1.30
5	4	12	8	0.5	12.	76.	1.3	21	2	1.35
6	3	10	8	0.5	12.	76.	1.3	21	3	1.35
7	3	10	8	0.5	12.	76.	1.3	21	4	1.35
8	3	10	10	0.5	12.	92.	1.3	21	3	1.35

potential models with no repulsion. Finally, our RSC results agree with the $^4a_{\rm nd}$ value of the Grenoble group (6.3 fm).

Next we examine the results for doublet Nd scattering lengths using the RSC model in the three-channel approximation. A selection of mesh parameters utilized in our study of accuracy and convergence is given in Table VI. The corresponding $^2a_{\rm nd}$ and $^2a_{\rm pd}$ values are compiled in Table VII. We concentrated on the pd scattering problem because it is more sensitive to mesh parameter variation. No essential differences were found between mesh requirements for the doublet scattering lengths and those previously discussed for the quartet scattering lengths. The RSC three-channel approximation seriously underbinds the triton (see Table III). Thus, it comes as no surprise that $^2a_{\rm nd}$ is larger than experiment and $^2a_{\rm pd}$ is even larger. The purpose of Table VII is to confirm that we have accurate, converged solutions.

Having investigated the quality of our zero-energy continuum solutions, we summarize our results for the trinucleon binding energies and Nd scattering lengths in Table VIII. The RSC three-channel Nd results are best estimates from Tables V and VII. The RSC five-channel doublet results provide an interesting comparison with the three-channel results: $^2a_{\rm nd}$ decreases much less than $^2a_{\rm pd}$, indicating that if $^2a_{\rm nd}$ is small enough, $^2a_{\rm pd}$ will be less than $^2a_{\rm nd}$. The V_{14} and SSCC models yield very similar values of $B(^3{\rm H})$; therefore, it is not surprising that the values of $^2a_{\rm nd}$ and $^2a_{\rm pd}$ for these models are quite comparable. The comparison of the quartet scattering lengths for all three models shows that $^4a_{\rm nd}$ is only slightly sensitive to the short-range repulsive nature of the potential model and the strength of the tensor force as characterized by the model value of $P_D(^2{\rm H})$. The values of $^4a_{\rm pd}$ are more sensitive to the off-shell differences of the potential models; the spread in $^4a_{\rm pd}$ values is three times that of the $^4a_{\rm nd}$ values. The RSC five-channel $^2a_{\rm nd}$ value agrees reasonably well with that of the Grenoble group[34] (1.6 fm) and the unitary pole approximation result of Afnan and Read[35] (1.8 fm). Our SSCC result for $B(^3{\rm H})$ agrees well with that of Ref. 35 (7.43 MeV), but our value of $^2a_{\rm nd}$ is somewhat smaller than theirs (1.52 fm). We do not understand this difference, in view of the reasonable agreement on $B(^3{\rm H})$ and for both RSC model results.

The results from Table VIII discussed above are interesting model results but do not speak directly to the issue raised in the Introduction. Do tensor force calculations confirm the conclusions, based upon the central force model, that $^4a_{\rm pd}$ should lie in the range 13.5—14.0 fm and that $^2a_{\rm pd}$ is very small? However, the last entry in Table VIII does address that issue. The entry RSC-5 [$1.11V(^1S_0)$] lists results for a calculation in which the spin-singlet potential is multiplied by the factor 1.11 in order to increase $B(^3{\rm H})$ to a value approximating the experimental triton binding energy (8.48 MeV). The corresponding value of $^2a_{\rm nd}=0.60$ fm is reasonably close to the experimental result (0.65 fm). The model value for $B(^3{\rm He})$ is larger than experiment, because the $B(^3{\rm H})-B(^3{\rm He})$ difference cannot be entirely accounted for by the Coulomb interaction between the two protons in ^{3}He.[36] However, we are interested here in the qualitative aspects of $^2a_{\rm pd}$, when the value of $^2a_{\rm nd}$ [and therefore $B(^3{\rm H})$] is essentially that observed experimentally. Thus, the value of $^2a_{\rm pd}=0.06$ fm for this modified RSC poten-

TABLE V. RSC model Nd quartet scattering lengths along with Kohn variational estimates and full Kohn pd estimates for mesh parameters listed in Table IV. Units are in fm.

Case	Channels	$^4a_{\rm nd}$	$^4a_{\rm nd}^K$	$^4a_{\rm pd}$	$^4a_{\rm pd}^K$	$^4a_{\rm pd}^{K,F}$
1	7	6.282	6.316			
1	5	6.281	6.314	13.291	13.335	13.527
1	3	6.282	6.315	13.296	13.340	13.530
1	2	6.282	6.316	13.297	13.341	13.531
2	2	6.288	6.313	13.312	13.344	13.534
3	2			13.315	13.344	13.534
4	2			13.312	13.344	13.534
5	2			13.312	13.344	13.534
6	2	6.294	6.313			
7	2	6.295	6.313			
8	2	6.303	6.305	13.334	13.340	13.530

TABLE VI. Mesh parameters employed in the accuracy and convergence study of the Nd doublet scattering length calculated using the RSC potential model in the three-channel approximation.

Case	N_I^ρ	N_M^ρ	N_E^ρ	$\rho_{\rm br}^I$	$\rho_{\rm br}^E$	$\rho_{\rm max}$	S_ρ	N_I^θ	N_E^θ	S_θ
1	4	10	6	0.5	12.	60.	1.30	20	2	1.30
2	4	10	6	0.5	12.	60.	1.30	17	3	1.30
3	4	10	6	0.5	12.	60.	1.30	19	2	1.30
4	4	10	7	0.5	12.	60.	1.30	19	2	1.30
5	4	10	7	0.5	12.	68	1.30	19	2	1.30
6	4	10	5	0.5	12.	60.	1.30	19	2	1.30
7	4	10	5	0.5	12.	52.	1.30	19	2	1.30
8	4	10	5	0.5	12.	52.	1.25	18	2	1.30
9	4	10	5	0.5	12.	52.	1.35	18	2	1.30
10	4	8	5	0.5	12.	52.	1.30	18	2	1.30
11	2	10	5	0.5	12.	52.	1.30	18	2	1.30
12	3	10	5	0.5	12.	60.	1.30	18	2	1.20
13	3	10	5	0.5	12.	60.	1.30	18	2	1.25
14	3	10	5	0.5	12.	60.	1.30	18	2	1.35
15	3	10	5	0.5	12.	60.	1.30	18	2	1.40
16	3	10	6	0.5	12.	60.	1.30	21	2	1.30
17	3	10	8	0.5	12.	76.	1.30	21	3	1.35
18	3	10	10	0.5	12.	92.	1.30	21	3	1.35

tial model does confirm the results reported previously[1] for a central force model. The results for the quartet scattering length from all three realistic potential models, already considered, clearly indicate that the theoretical range for ${}^4a_{\rm pd}$ is 13.5—14.0 fm, when higher partial waves are included (Δ^4a^K being about 0.2 fm in each case).

IV. DOUBLET SCATTERING LENGTH VERSUS TRINUCLEON BINDING ENERGY

The results for the RSC model summarized in Table VIII are very suggestive. Although the relationship between $B({}^3\text{H})$ and ${}^2a_{\rm nd}$ has been described as linear, it seems clear that the relationship is not so simple when one examines a broader region than that immediately adjacent to the experimental value (8.48 MeV and 0.65 fm). In particular, the value of ${}^2a_{\rm pd}$ decreases much more rapidly than does that of ${}^2a_{\rm nd}$ as one moves from the RSC three-channel model to the RSC five-channel model to the RSC $[1.11V({}^1S_0)]$ five-channel model.

TABLE VII. RSC three-channel Nd doublet scattering length results along with Kohn variational estimates and full Kohn pd estimates for mesh parameters listed in Table VI. Units are in fm.

Case	${}^2a_{\rm nd}$	${}^2a_{\rm nd}^K$	${}^2a_{\rm pd}$	${}^2a_{\rm pd}^K$	${}^2a_{\rm pd}^{K,F}$
1			3.450	3.454	3.322
2			3.119	3.456	3.324
3			3.435	3.454	3.323
4			3.435	3.454	3.232
5			3.432	3.451	3.319
6			3.434	3.454	3.323
7			3.446	3.465	3.334
8			3.382	3.466	3.335
9			3.383	3.466	3.335
10			3.385	3.468	3.337
11			3.383	3.471	3.339
12			1.021	3.539	3.403
13			2.563	3.465	3.333
14			3.451	3.455	3.323
15			3.458	3.457	3.325
16			3.452	3.454	3.323
17	2.339	2.340	3.452	3.450	3.318
18	2.341	2.337	3.462	3.448	3.316

To investigate this further, we have generated the curves for $B({}^3\text{H})$ vs ${}^2a_{\rm nd}$ and $B({}^3\text{He})$ vs ${}^2a_{\rm pd}$ by keeping the ${}^3S_1$-${}^3D_1$ potential unaltered (so as to fix the deuteron pole properties) and varying the overall strength of the spin-singlet (${}^1S_0$) potential. The trinucleon binding energies and Nd doublet scattering lengths were calculated using the RSC potential model in the three-channel approximation. (The three-channel approximation was used for simplicity.) The resulting curves are displayed in Fig. 1. The five-channel results for each of the three models investigated in this paper are shown also. These five-channel points fall on the curves, validating our use of the three-channel RSC model to generate the curves.

It is obvious that the relationship between $B({}^3\text{H})$ and ${}^2a_{\rm nd}$ is not linear except in the region near the experimental value. It is not so obvious, because of the Coulomb shift in the binding energy, that the Coulomb correction to the doublet scattering length vanishes around ${}^2a_{\rm Nd}=1.3$ fm. Thus we find that if ${}^2a_{\rm nd}>1.3$ fm, then ${}^2a_{\rm pd}$ will be even larger. [This is the situation one finds for most "realistic" local nucleon-nucleon potential model calculations where $B({}^3\text{H})<7.5$ MeV.] Conversely, if ${}^2a_{\rm nd}<1.3$ fm, then ${}^2a_{\rm pd}$ will be smaller than ${}^2a_{\rm nd}$. (This is the physical situation where ${}^2a_{\rm nd}\cong 0.65$ fm.) Specifically, we find from this model study that ${}^2a_{\rm pd}\cong 0$ is predicted because the experimental ${}^2a_{\rm nd}$ is measured to be some 0.65 fm.

The curves in Fig. 1 are similar in shape to the two-body plots of Refs. 1 and 37 which showed the Coulomb and non-Coulomb scattering lengths as a function of the overall strength of the potential. In the Appendix of Ref. 1, we explored via perturbation theory the expansion

TABLE VIII. Summary of the trinucleon binding energies and nucleon-deuteron scattering lengths for the four tensor force models investigated. $\Delta^4 a_{\rm pd}^K$ is the additional quartet pd scattering length from the $a_{\rm pd}^{K,F}$ calculation.

Model	$B(^3\mathrm{H})$ (MeV)	$^2a_{\rm nd}$ (fm)	$^4a_{\rm nd}$ (fm)	$B(^3\mathrm{He})$ (MeV)	$^2a_{\rm pd}$ (fm)	$^4a_{\rm pd}$ (fm)	$\Delta^4 a^K$ (fm)
RSC-3	6.38	2.34		5.77	3.46		
			6.30			13.33	0.20
RSC-5	7.02	1.76		6.39	2.23		
V_{14}	7.44	1.35	6.38	6.80	1.42	13.57	0.19
SSCC	7.46	1.32	6.41	6.81	1.35	13.67	0.17
RSC-5 $[1.11V(^1S_0)]$	8.56	0.60		7.89	0.06		

$$\frac{1}{a_c}=\frac{\lambda}{a}+\delta$$
$$=\frac{1}{a}+\xi\epsilon+\xi(\ln\xi+2\gamma)\,,$$

where γ is Euler's constant and $\xi=2\mu\alpha c/\hbar$ depends upon the reduced mass, μ, and the fine structure constant, α. We point out here that it is $\xi(\ln\xi+2\gamma)\sim 1/(10\text{ fm})$ that provides the scale that separates long range from short range in the Coulomb problem. Thus, it is the long-range effects that are of primary importance in modifying the nn scattering length from -17 to -7.8 fm in the pp system. In addition, one has

$$\lambda-1=-2\xi\int_0^\infty [1-g(r)]dr\,,$$

where $g(r)$ is the short range defect function in the s-wave scattering length wave function, $\phi(r)=r-ag(r)$. The $g(r)$ approaches [0,1] as $r\to[0,\infty]$, so that $\int_0^\infty [1-g(r)]dr>0$ and $\lambda<1$ if $g(r)$ approaches its asymptotic value from below; conversely, $\lambda>1$ if it approaches from above. Large values of the scattering length a correspond to the former case, while small values correspond to the latter case. Thus, we find $\lambda>1$, which accounts for $^2a_{\rm pd}<{}^2a_{\rm nd}$ for small values of $^2a_{\rm Nd}$.

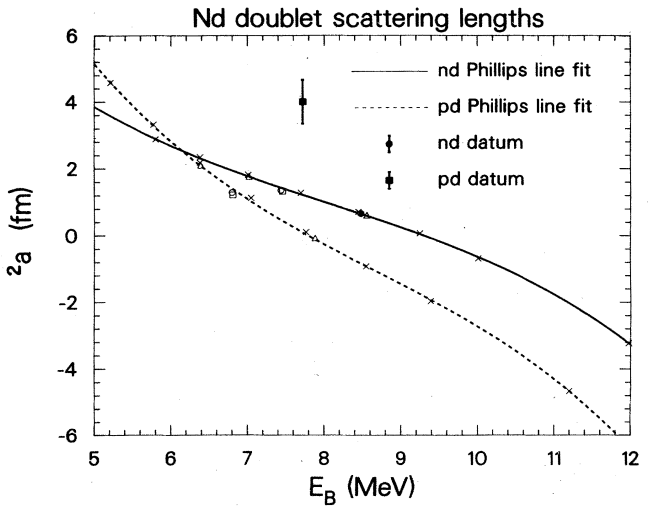

FIG. 1. The nd doublet scattering length versus the trinucleon bound state energy: the solid curve describes the nd-^{3}H system and the dashed curve describes the pd-^{3}He system. The $\times$'s are the RSC points calculated as a function of the strength of the $^1S_0$ potential. The open symbols correspond to the five-channel results from Table VIII: Δ represents RSC, $\circ$ represents V_{14}, $\square$ represents SSCC.

V. CONCLUSIONS

We have calculated the Coulomb modified strong interaction pd scattering lengths using our configuration space formulation of the Faddeev equations. Our results for the three tensor force models considered (the RSC, the V_{14}, and the SSCC) are in essential agreement with the central force results which we obtained previously. In particular, we find that $^4a_{\rm pd}$ is expected to lie in the range 13.5—14.0 fm and that $^2a_{\rm pd}$ is predicted to be essentially 0 fm. The first result is some 2 fm larger than the presently accepted experimental value. The second result is in clear disagreement with the quoted measurement. Furthermore, it disagrees qualitatively with the approximate theoretical calculations which predict $^2a_{\rm pd}>{}^2a_{\rm nd}$. However, we have investigated the relation between trinucleon binding energy and doublet scattering length. We find it to be nonlinear, and we find that it supports our conclusion that experimentally $^2a_{\rm pd}\ll{}^2a_{\rm nd}$.

As we have stated previously, low-energy pd cross sections are difficult to measure because of the Gamow factor suppression. In addition, it was the case in nd scattering that very low-energy measurements were required, before the correct $^2a_{\rm nd}$ and $^4a_{\rm nd}$ values could be extracted from the data. Thus, we hope to stimulate further experimental effort to measure these fundamental properties of the pd system. On the theoretical side, it seems clear that three-body force effects must be included. The theoretical model of the three-nucleon system should reproduce the measured trinucleon properties before one can be certain that the conclusions reached here are completely correct.

ACKNOWLEDGMENTS

B.F.G. acknowledges several useful conversations with D. R. Lehman on Coulomb problems. The work of J.L.F. and B.F.G. was performed under the auspices of the U. S. Department of Energy; the work of G.L.P. and C.R.C. was supported in part by the U. S. Department of Energy.

[1]J. L. Friar, B. F. Gibson, and G. L. Payne, Phys. Rev. C **28**, 983 (1983).
[2]A. C. Phillips, Phys. Rev. **142**, 984 (1966); see also A. C. Phillips and G. Barton, Phys. Lett. **28B**, 378 (1969).
[3]G. L. Payne, J. L. Friar, and B. F. Gibson, Phys. Rev. C **26**, 1385 (1982).
[4]E. O. Alt, in *Proceedings of the VIIth International Conference on Few Body Problems in Nuclear and Particle Physics,* edited by A. N. Mitra, I. Slaus, V. S. Bashin, and V. K. Gupta (North-Holland, Amsterdam, 1976), p. 76.
[5]A. C. Phillips, Rep. Prog. Phys. **40**, 905 (1977).
[6]W. Dilg, L. Koester, and W. Nistler, Phys. Lett. **36B**, 208 (1971).
[7]R. S. Christian and J. L. Gammel, Phys. Rev. **91**, 100 (1953).
[8]L. M. Delves, Phys. Rev. **118**, 1318 (1961).
[9]W. T. H. van Oers and K. W. Brockman, Jr., Nucl. Phys. **A92**, 561 (1967); W. T. H. van Oers and J. D. Seagrave, Phys. Lett. **24B**, 562 (1967).
[10]A. S. Reiner, Phys. Lett. **28B**, 387 (1969).
[11]S. K. Adhikari and J. R. A. Torreão, Phys. Lett. **119B**, 245 (1982).
[12]P. Stoler, N. N. Kaushal, F. Green, E. Harms, and L. Laroze, Phys. Rev. Lett. **29**, 1745 (1972); P. Stoler, N. N. Kaushal, and F. Green, Phys. Rev. C **8**, 1539 (1973).
[13]E. Huttel, W. Arnold, H. Baumgart, H. Berg, and G. Clausnitzer, Nucl. Phys. **A406**, 443 (1983).
[14]J. Arvieux, Nucl. Phys. **A221**, 253 (1974).
[15]W. Timm and M. Stingl, J. Phys. G **2**, 551 (1976).
[16]D. Eyre, A. C. Phillips, and F. Roig, Nucl. Phys. **A275**, 13 (1977); D. Eyre and A. C. Phillips, *ibid.* **A275**, 29 (1977).
[17]Y. Avishai and A. S. Rinat, Phys. Lett. **36B**, 161 (1971).
[18]E. O. Alt, P. Grassberger, and W. Sandhas, Nucl. Phys. **B2**, 167 (1967).
[19]A. A. Kvitsinski, Pis'ma Zh. Eksp. Teor. Fiz. **36**, 375 (1982) [JETP Lett. **36**, 454 (1983)].
[20]H. Zankel and L. Mathelitsch, Phys. Lett. **132B**, 27 (1983).
[21]W. Kohn, Phys. Rev. **74**, 1763 (1948); S. P. Merkuiev, Nucl. Phys. **A283**, 395 (1974); J. Nuttal, Phys. Rev. Lett. **19**, 473 (1967); for further references, see R. J. Nesbet, *Variational Methods in Electron-Atom Scattering* (Plenum, New York, 1980).
[22]L. D. Faddeev, Zh. Eksp. Teor. Fiz. **39**, 1459 (1960) [Sov. Phys.—JETP **12**, 1014 (1961)].
[23]H. P. Noyes, in *Three Body Problem in Nuclear and Particle Physics,* edited by J. S. C. McKee and P. M. Rolph (North-Holland, Amsterdam, 1970), p. 2.
[24]J. J. Benayoun and C. Gignoux, Nucl. Phys. **A190**, 419 (1972); A. Laverne and C. Gignoux, *ibid.* **A203**, 597 (1973); S. P. Merkuriev, C. Gignoux, and A. Laverne, Ann. Phys. (N.Y.) **99**, 30 (1976).
[25]E. F. Redish, in *Few Body Systems and Nuclear Forces II, Lecture Notes in Physics,* edited by H. Zingl, M. Haftel, and H. Zankel (Springer, Berlin, 1978), Vol. 87, p. 427.
[26]T. Sasakawa and T. Sawada, Phys. Rev. C **20**, 1954 (1979).
[27]J. L. Friar, B. F. Gibson, D. R. Lehman, and G. L. Payne, Phys. Rev. C **25**, 1616 (1982).
[28]S. P. Merkuriev, Yad. Fiz. **23**, 6 (1976) [Sov. J. Nucl. Phys. **23**, 141 (1976)].
[29]G. L. Payne, J. L. Friar, B. F. Gibson, and I. R. Afnan, Phys. Rev. C **22**, 823 (1980).
[30]P. M. Prenter, *Splines and Variational Methods* (Wiley, New York, 1975).
[31]R. V. Reid, Ann. Phys. (N.Y.) **50**, 411 (1968).
[32]R. B. Wiringa, R. A. Smith, and T. L. Ainsworth, Phys. Rev. C **29**, 1207 (1984).
[33]R. de Tourreil and D. W. L. Sprung, Nucl. Phys. **A201**, 193 (1973).
[34]J. J. Benayoun, C. Gignoux, and J. Chauvin, Phys. Rev. C **23**, 1854 (1981).
[35]I. R. Afnan and J. M. Read, Phys. Rev. C **12**, 293 (1975).
[36]J. L. Friar and B. F. Gibson, Phys. Rev. C **18**, 908 (1978).
[37]J. L. Friar, B. F. Gibson, and G. L. Payne, Phys. Lett. **124B**, 287 (1983).